Title

EFFECTS OF STEAM-LIQUID COUNTERFLOW ON PRESSURE TRANSIENT DATA FROM TWO-PHASE GEOTHERMAL RESERVOIRS

Authors

Bodvarsson, G.S.
Cox, B.L.
Ripperda, M.

Publication Date

1987-06-01

LBL-23719

Lawrence Berkeley Laboratory
UNIVERSITY OF CALIFORNIA

EARTH SCIENCES DIVISION

Presented at the 62nd Annual Technical Conference and Exhibition of the Society of Petroleum Engineers, Dallas, TX, September 27–30, 1987, and published in the Proceedings

Effects of Steam-Liquid Counterflow on Pressure Transient Data from Two-Phase Geothermal Reservoirs

G.S. Bodvarsson, B.L. Cox, and M. Ripperda

June 1987

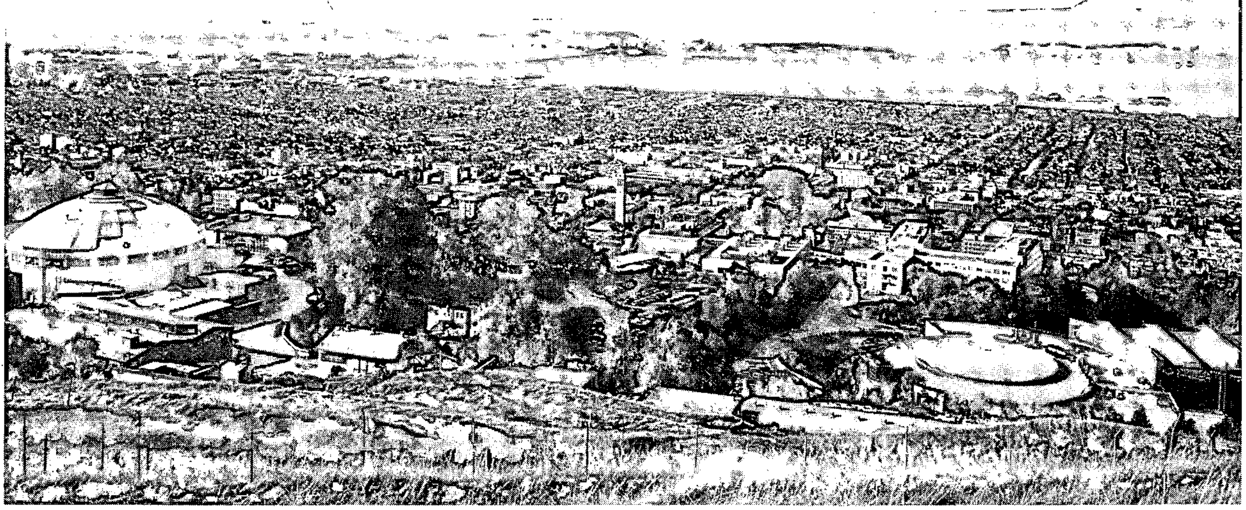

Prepared for the U.S. Department of Energy under Contract DE-AC03-76SF00098

DISCLAIMER

LBL-23719

Effects of Steam-Liquid Counterflow on Pressure Transient Data from Two-Phase Geothermal Reservoirs

G.S. Bodvarsson, B.L. Cox, and M. Ripperda
Lawrence Berkeley Laboratory
University of California
Berkeley, California 94720

ABSTRACT

Numerical studies are performed to investigate the effects of localized feedzones on the pressure transients in two-phase reservoirs. It is shown that gravity effects can significantly affect the pressure transients, because of the large difference in the density of liquid water and vapor. Production from such systems enhances steam/liquid water counterflow and expands the vapor-dominated zone at the top of the reservoir. Subcooled liquid regions develop in the center of the reservoir due to gravity drainage of cooler liquid water. The vapor zone will act as a constant pressure boundary and help stabilize the pressure decline in the system. It is shown that the pressure transients at observation wells depend greatly on the location (depth) of the major feedzone; if this is not accounted for, large errors in deduced reservoir properties will result. At shallow observation points pressures may actually increase as a result of enhanced steam upflow due to production at a deep feedzone.

INTRODUCTION

In two-phase geothermal reservoirs heat is transported from the reservoir bottom to the caprock through counterflow of liquid and steam, often referred to as the heat pipe effect (White et al., 1971). Because the heat content per unit mass of steam is much higher than that of liquid water at the same temperature, a mass-balanced counterflow of the two phases will result in heat transport to the caprock from below. A given heat throughflow can give rise to two different thermodynamic conditions in the reservoir; one where the vapor phase is nearly immobile and the pressure gradient is slightly less than hydrostatic, and the second one where the liquid phase is nearly immobile and the pressure gradient slightly exceeds vaporstatic conditions (Martin et al., 1976). In both cases the product of the pressure gradient and the fluid mobility will be equal for the two phases, resulting in a mass-balanced counterflow. In this paper a reservoir with a liquid-dominated heat pipe is considered; i.e., the initial pressure gradient in the reservoir is near-hydrostatic.

References and illustration at end of paper.

Most geothermal reservoirs are located in fractured rocks, with fluids entering the wellbore where it intersects major faults and fractures. These points are commonly referred to as feedzones. Most geothermal wells have one or two major feedzones, the locations of which are inferred from drilling data (lost circulation, drilling rates), pressure and temperature profiles during heating of the well after drilling, and spinner tests during cold water injection tests (most spinners are not operational at the high temperatures encountered in many geothermal wells). The pressure transients for systems with localized feedzones have received little attention, with the exception of studies addressing partially penetrating wells (Witherspoon et al., 1967; Earlougher, 1977). The available results for partially penetrating wells are not readily applicable to problems involving fractured, two-phase reservoirs, because it is assumed that the open well interval is at the top of the reservoir, and important gravity effects associated with two-phase reservoirs are neglected.

Production results in pressure decline around well feedzones, which enhances vapor saturation. The increase in vapor saturation disturbs the stable counterflow mechanism. This will enhance steam upflow and cause a steam zone to develop at the top of the reservoir beneath the caprock. Furthermore, gravity effects will cause liquid downflow from shallow reservoir regions to the depth of the feedzone. These effects combine to produce complex pressure transients that will yield erroneous results when conventional methods of analysis are employed.

Some studies have been conducted on presure transients in two-phase reservoirs, generally neglecting gravity effects and localized feedzones. Various investigators have extended the single-layer pressure transient theory to two-phase systems (Grant, 1978; Garg, 1978; O'Sullivan, 1980; Sorey et al., 1980). These investigators incorporated the effects of the fluid enthalpy in their methods of analysis, but rigorous analysis is still not possible due to lack of knowledge regarding relative permeabilities (Grant, 1980). Moench (1978) and Moench and Atkinson (1978) investigated pressure transients in two-phase fractured reservoirs with immobile liquid water. Cox and

Bodvarsson (1985) investigated the effects of localized two-phase zones on pressure transient data. They included gravity effects in some of the cases and illustrated that they can have large effects on the pressure transients.

The main objective of this paper is to investigate the importance of gravity effects and localized fluid production (partial penetration) on the pressure behavior of two-phase reservoirs. The pressure transients at production wells are investigated as well as the pressure behavior of observation wells. Of particular interest are the pressure transients at observation wells with feedzones at different depths. These data can help evaluate steam/liquid water counterflow and horizontal and vertical permeabilities. The global changes in thermodynamic conditions of two-phase reservoirs during localized production are also investigated in order to understand the long term behavior of such systems.

APPROACH

The reservoir system considered is shown in Figure 1. A single well penetrates a two-phase reservoir; production from the well is assumed to be either from the top or bottom of the reservoir. The reservoir is 500 m thick and the production interval is assumed to be 50 m thick. A ten-layer grid is used, each layer being 50 m thick. A constant mass flow rate of 15 kg/s is specified for the well.

Initially, two-phase conditions prevail everywhere in the reservoir system. Two-phase conditions with nearly uniform vapor saturation ($S_v \approx 0.05$) were achieved by maintaining an appropriate heat flow through the system (Martin et al., 1976). Constant heat flux is applied at the bottom and the energy is transferred to the top of the reservoir by liquid-vapor counterflow. A constant heat sink is specified at the top of the reservoir, representing conductive heat losses. The heat flux used was 0.4 W/m^2, which results in a vapor liquid counterflow of approximately 2.4 x 10^{-7} kg/s m^2. The initial pressure is practically hydrostatic with depth, and the initial temperature in the top and bottom layers is 245 and 287 °C, respectively.

A porous-medium model is employed in this work, as it appears reasonable to attempt to understand porous medium behavior before tackling the more complex case of a fractured reservoir. The porosity and horizontal permeability in the system are assumed to be 5% and 50 md, respectively; the vertical permeability is varied in the simulations. Linear relative permeabilities are used, with an immobile liquid saturation of 0.40 and immobile vapor saturation of 0.05. The numerical simulator MULKOM (Pruess, 1982) is used in this work.

PRODUCTION FROM DEEP FEED ZONES

A number of cases are simulated with fluids produced from the bottom 50 m of the reservoir. Figure 2 shows the simulated pressure transient results at the well for various vertical permeabilities of the reservoir rocks. The figure shows, as expected, that the lower the vertical permeability the larger the pressure decline. The pressure decline is near-linear at early times and the slope of the line can be used to calculate the permeability-thickness of the producing layer, providing that proper enthalpy corrections are made (Grant, 1980). At later times the pressure decline stabilizes, as fluids from above recharge the producing layer. This pressure response resembles that from leaky aquifers (Hantush, 1960). However, the subsequent rise in pressure is not consistent with leaky aquifer solutions, but can be explained by transients in the enthalpy of the produced fluids shown in Figure 3. Figure 3 shows that after an initial stabilization in the flowing enthalpy at approximately 1500 kJ/kg, it decreases to about 1250 kJ/kg, which is practically the liquid enthalpy corresponding to the initial temperature of the producing layer (287 °C). The decrease in enthalpy is due to liquid recharge from above; the near-hydrostatic pressure gradient in the system does not allow downward flow of vapor. This in turn causes an increase in pressure at the well because an increase in the liquid fraction of the flowing fluids enhances the overall mobility of the mixture.

Log-log plots of the pressure transients at various observation points in the producing layer are shown in Figure 4 for the case of isotropic permeabilities. The curves show similar characteristics to those observed at the well and much more pressure stabilization than could be explained using a leaky aquifer solution. The characteristic shape of the curves closely resembles those obtained for a system with a constant pressure zone. However, evaluation of the pressure transients using such models will yield erroneous estimates for the hydrological parameters of the system.

The pressure transients for observation points at the top of the reservoir system exhibit more unorthodox behavior, as shown in Figure 5. Pressure transient data are given for observation wells located at different radial distances from the producing well. Figure 5 shows that the pressure actually increases at the top of the reservoir due to steam upflow from depth and condensation in the shallow regions. The condensation causes a temperature rise and consequently a pressure increase. The shorter the distance between the producing well and the observation point, the more pronounced the pressure rise. The pressure rise certainly also depends upon the effective vertical permeability of the vapor phase as well as the production rate of the well. The data shown in Figure 5 were computed for the case of isotropic permeability, but pressure increases were also observed for the cases with an anisotropy of 10 and 100. Here anisotropy is defined as the ratio of horizontal to vertical permeability. Pressure increases in shallow two-phase zones due to deeper production have been observed in several geothermal fields, for example, the Svartsengi geothermal field in Iceland (V. Stefansson, personal communication, 1982).

The pressure transient data shown in Figure 5 illustrate that very little if any pressure decline is observed at the top of the reservoir system during the entire time modeled (30 years). Thus, the pressure stabilization seen at the observation points at the bottom of the reservoir (Fig. 4) can be explained by the constant pressure zone at the top of the reservoir system. In order to explain the lack of pressure drawdown at the top of the reservoir one must consider the depletion patterns that evolve during production. Figure 6 shows the vapor saturation distribution in the system at the end of the simulation period (30 years). The figure shows that the fluid depletion occurs primarily at the top of the reservoir, where a steam-dominated zone has developed. In the lower part of the reservoir, in the vicinity of the well, two-phase conditions have disappeared and subcooled liquid is present. Farther from the well, the initial thermodynamic conditions prevail with vapor saturations close to 0.05. Apparently, during production from the bottom layer the pressure declines until it evokes significant vertical recharge. Gravity drainage becomes the dominating flow mechanism, causing an expanding steam zone to form at the top of the reservoir system. Little localized boiling occurs at the top of the reservoir so that temperatures and consequently pressures are maintained. Lateral flow of steam in the vapor-dominated zone will also help maintain temperatures and pressures (Cox and Bodvarsson, 1986).

The development of the subcooled liquid zone (see Fig. 6) is also an interesting consequence of the flow patterns that develop in the system. Two-phase conditions disappear in this zone because of downward flow of cooler liquid water from shallower portions of the reservoir. Figure 7 shows the total temperature changes in the system after 30 years of production. Downward flow of cooler liquid water has caused considerable cooling has occurred in the near region of the well (to a radial distance of about 300 m). It is only in the bottom layer (the producing layer) that a significant temperature drop due to boiling has occurred.

It is of interest to investigate how the pressure transient behavior of the system at observation wells changes from the near-constant pressure behavior in the expanding steam zone at the top of the reservoir to the "Theis-like" behavior at the bottom of the reservoir. Figures 8 and 9 show the pressure and vapor saturation transients, respectively, observed at 80 m from the well for four different locations in the reservoir (10, 50, 325 and 475 m below the caprock). Note that these figures were developed using a finer grid at the upper 100 m of the reservoir (20 m grid) and a production rate of 10 kg/s. These figures show several interesting points. Figure 8 shows that if the depth of the observation point is more than 300 m below the caprock for the system considered, the pressure transients will show a temporary pressure decline followed by a recovery although fluids are constantly being produced at the well. The late time recovery is due to the vertical liquid drainage that provides pressure support. At observation points less than 300 m below the caprock, the effects of steam upflow enhanced by production are felt. At early times, pressures usually rise due to steam upflow and condensation. At late times, however, the liquid drainage dominates, causing the pressure to assympototically decline to the initial pressure. This pressure decline is limited because of the stable pressures in the steam zones. For observation points that undergo transition from liquid-dominated to vapor-dominated conditions (the observation point 10 m below the caprock), the pressure transients are substantially different from those observed in the liquid-dominated zone. For these observation points, pressures initally decline, until immobile liquid conditions are reached (liquid drainage period). After that pressures increase rapidly due to steam upflow from depth and condensation. However, the pressure rise is only temporary because of two factors; the readily mobile steam phase in the expanding vapor zone will rapidly equilibrate pressures, and the increasing liquid downflow will quench the steam upflow from depth. The gradual advancement of the steam bubbles from depth into various layers is clearly demonstrated in Figure 9.

It is also of interest to investigate how the general flow patterns and thermodynamic conditions change with decreasing vertical permeability, since for many geothermal systems the vertical permeability is considerably lower than the horizontal permeability. Figure 10 shows the distribution in vapor saturation for the same system, but with a vertical permeability ten times lower (anisotropy of 10). The results show the same general trends as those obtained in the isotropic permeability case, that is, fluid depletion at shallow depths and the presence of a subcooled liquid zone. In this case, however, the vapor dominated zone and the subcooled liquid zone extend farther from the well (over a larger reservoir volume). The greater extent of these zones is caused by the larger pressure drop (see Fig. 2), resulting from the lower vertical permeability.

Similar results were obtained for the case with an anisotropy of 100. However, when anisotropy was assumed to be 10^4, little vertical leakage occurred. Therefore, all of the reservoir remains two-phase for the entire simulated period. Near the production interval significant boiling occurred and an expanding vapor-dominated zone formed.

In summary, Figure 11 shows the resulting model of fluid flow patterns and reservoir depletion for a well with a deep feedzone. It is assumed for this model that there is sufficient vertical permeability to cause shallow reservoir depletion rather than localized boiling around the well feedzone. The production rate and the anisotropy ratio determine the radius of influence for this system, and gravity drainage provides a very efficient production (depletion) mechanism.

In the model shown in Figure 11, vertical flow is dominant, and one should therefore be able to estimate the average vertical permeability from pressure transient data for such systems. As mentioned before, the early pressure transients in the well and at nearby observation points can be used to determine the average horizontal transmissivity of the production layer. The later time pressure transient data are mostly affected by the vertical liquid flow and the development of the near-constant pressure vapor-dominated zone at the top of the system. Figure 12 shows the correlation between the stabilized well pressures and the anisotropy ratio.

As shown in the figure a log-linear correlation is obtained. Such a correlation between these parameters is expected for linear problems, but is rather surprising for this more complex non-linear problem. However, the fluids flowing in the reservoir system are predominately liquid water and gravity drainage rather than boiling causes the reservoir depletion. Hence, relative permeability effects are small.

It may also be possible to estimate the average vertical permeability of steam (kk_{rs}) from the pressure increase at shallow observation points (Fig. 4). This pressure increase is due to upflow of steam and condensation at the top of the reservoir system. The pressure change can be used to estimate the temperature change at the top of the reservoir, and the temperature change can in turn be used to infer the amount of steam that has condensed. Averaging the total amount of steam over the time period of the pressure rise, the average rate of steam upwelling may be determined; this steam rate can then be used to estimate the average vertical permeability to steam (kk_{rv}). This effective steam permeability is:

$$kk_{rv} = \frac{\mu_v}{\rho_v} \frac{\rho_a c_a (\Delta T \Delta z)_{tot}}{\rho_l \, g t h_v} \tag{1}$$

Where μ_v and ρ_v are the $\rho_a c_a$ is the total fluid rock volumetric ρ_l is the liquid density, g is the gravitational constant, t is time and h_v is the enthalpy of vapor. The term $(\Delta T \Delta z)_{tot}$ is the total temperature change at the top of the reservoir integrated over the vertical extend of the temperature rise. This term causes the most difficulty in obtaining estimate for kk_{rv}, and requires pressure data from several observation wells with shallow feedzones at different elevations.

PRODUCTION AT TOP OF RESERVOIR

Several cases were simulated with fluid production at the top of the reservoir (see Fig. 1). Again a constant fluid production of 15 kg/s is specified. Figure 13 shows the pressure transients at the production interval for cases with different vertical permeability (anisotropy). Comparison of the results shown in Figure 13 with those of Figure 2 indicates that for the same production rate the pressure decline is considerably higher for the shallow production case. This is caused by gravity effects, which enhance recharge to a well with a deep feedzone, but oppose upward recharge of liquid water in the case of shallow production. However, the large pressure decline during shallow production overcomes the gravity effects and evokes significant upward recharge of liquid water. This liquid recharge reduces the enthalpy of the produced fluids as shown in Figure 14, and the pressure decline stabilizes.

As was observed for the case of deep production, the pressure decline for the various vertical permeabilities is also approximately a linear function of the logarithm of the anisotropy for the shallow production case (Fig. 13). Figure 15 shows the pressure transients for various observation points in the shallow production layer for the case with isotropic permeability. As expected the pressures stabilize at late times in the observation wells due to the recharge from depth. We attempted to fit these data to type curves based upon a partial penetration model using the appropriate geometrical constants ($r/H = 0.33$, $L/H = 0.2$, $z/H = 0.10$). As shown in Figure 16 the type curve does not match the entire data set very well, as the simulated data show more pressure stabilization than do the type curves. The pressure stabilization is due primarily to upflow of steam and condensation in the shallow production layer. The match with the early time data gives reasonable estimates of the transmissivity of the shallow production layer; the match with the later time data yields transmissivity values that are too high. Figure 17 shows the pressure transients for various observation points at the bottom of the system. These data are again generated for the isotropic reservoir case, and as shown in the figure, the data can be matched reasonably well using the Theis type curve. Surprisingly, the resulting transmissivity values agree reasonably well with the overall transmissivity of the system ($2.5 \times 10^{-11}\ m^3$). For the cases with anisotropy the pressure transients are much more complex and can not be analyzed using any of the available type curves.

CONCLUSIONS

Numerical simulation methods are used to investigate gravity effects on pressure transient data and depletion patterns in two-phase reservoirs. The studies show that both gravity effects and production from localized feedzones can have significant effects upon the pressure transient data. The following general conclusions can be made:

(1) Production from a deep feedzone gives rise to an efficient gravity drainage mechanism that causes only gradual long-term pressure changes at the well.

(2) If the vertical permeability is significant, (more than four orders of magnitude less than the horizontal permeability for the cases studied), reservoir depletion primarily takes place at the top of the reservoir, with the development of an expanding steam-dominated zone.

(3) The pressures in the steam-dominated zone remain relatively constant during the production period simulated, resulting in a leveling of the pressure decline at observation points (wells). However, at early times pressures may actually increase at shallow depth due to upflow of steam and condensation.

(4) Production from deep feedzones evokes recharge of cooler fluids from shallow regions, and a subcooled liquid-dominated zone develops in the middle of the reservoir system.

(5) Production from shallow feeds results in considerably higher pressure drops than those from deeper zones, because of gravity effects.

(6) Upward flow of liquid reduces enthalpies in the produced fluids, and stabilizes pressures more than would be expected based upon the partial penetration theory.

(7) The studies presented here are preliminary. It appears that more research in these areas would increase our understanding of complex fractured reservoirs and consequently lead to more efficient development plans.

ACKNOWLEDGMENTS

The authors express their gratitude to S. Benson and S. Gaulke for technical review of this manuscript and to K. Pruess for allowing use of the MULKOM code for this study. This work was supported through U.S. Department of Energy Contract No. DE-AC03-76SF00098 by the Assistant Secretary for Conservation and Renewable Energy, Office of Renewable Technology, Division of Geothermal Technology.

REFERENCES

Cox, B. L. and Bodvarsson, G. S., 1985. Preliminary studies of two-phase effects on pressure transient data, Proc. Geothermal Reservoir Engineering Workshop, Vol. 11, Stanford University, in press.

Earlougher, Jr., R. C., 1977. Advances in Well Test Analysis, Society of Petroleum Engineers, Monograph 5.

Garg, S. K., 1978. Pressure transient analysis for two-phase (liquid water/steam) geothermal reservoirs, *Soc. Petr. Eng. Journal*, Vol. 20, No. 6, pp. 206-214.

Grant, M. A., 1978. Two-phase linear geothermal pressure transients: A comparison with single-phase transients, *New Zealand Journal of Science*, Vol. 21, pp. 355-364.

Grant, M. A., 1980. The testing of KA28-pressure analysis in a two-phase reservoir, Proc. Geothermal Reservoir Engineering Workshop, Vol. 6, Stanford University, pp. 170-177.

Hantush, M. S., 1960. Modification of the theory of leaky aquifers, *Journal Geophysical Research*, Vol. 56, p. 3713.

Martin, J. C., Wegner, R. E. and Kelsey, F. J., 1976. One dimensional convective and conductive geothermal heat flow, Proc. Geothermal Reservoir Engineering Workshop, Vol. 2, Stanford University, pp. 251-261.

Moench, A., 1978. The effects of thermal conduction upon pressure drawdown and buildup in fissured vapor-dominated geothermal reservoirs, Proc. Geothermal Reservoir Engineering Workshop, Vol. 4, Stanford University, pp. 112-117.

Moench A. F. and Atkinson, P. G., 1978. Transient pressure analysis in geothermal steam reservoirs with an immobile vaporising liquid phase, *Geothermics*, Vol. 7, pp. 253-264.

O'Sullivan, M. J., 1981. A similarity method for geothermal well test analysis, *Water Resources Research*, Vol. 17, No. 2, pp. 390-398.

Pruess, K., 1982. Development of the general purpose simulator MULKOM, 1982 Annual Report, Earth Sciences Division, Lawrence Berkeley Laboratory, Berkeley, CA, p. 133-134.

Witherspoon, P. A., Javandel, I., Neuman, S. P. and Freeze, R. A., 1967. Interpretation of Aquifer Gas Storage Conditions from Water Pumping Tests, American Gas Association Monograph, New York, 273 pp.

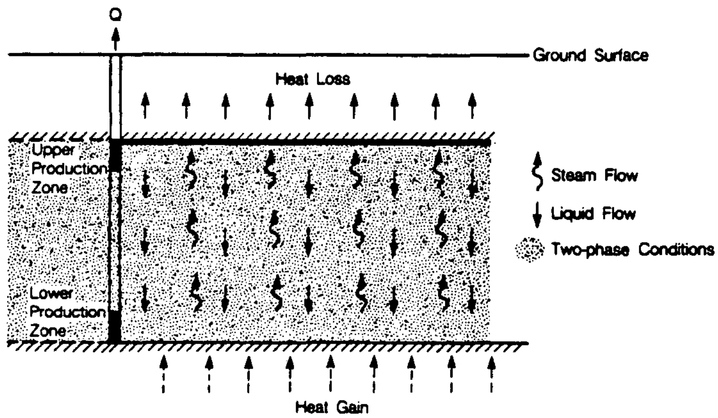

Fig. 1—Basic model used in the simulation studies. A stable two-phase zone is achieved by heat flow through the reservoir.

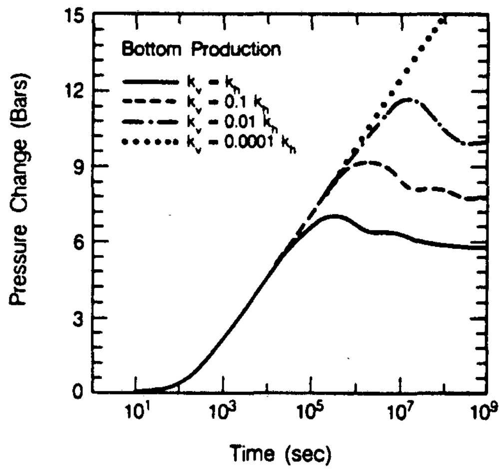

Fig. 2—Pressure decline at the well, when fluids are produced from a deep feed zone. Different vertical permeabilities are used.

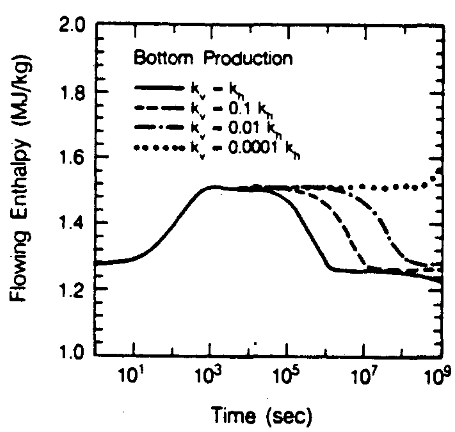

Fig. 3—Flowing enthalpy of the produced fluids for deep production and various values of the vertical permeability.

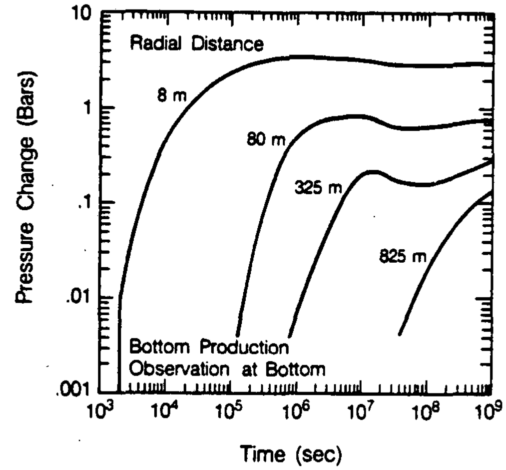

Fig. 4—Pressure transients in deep observation points at different radial distances from the well. Fluids are produced from the deep feed zone.

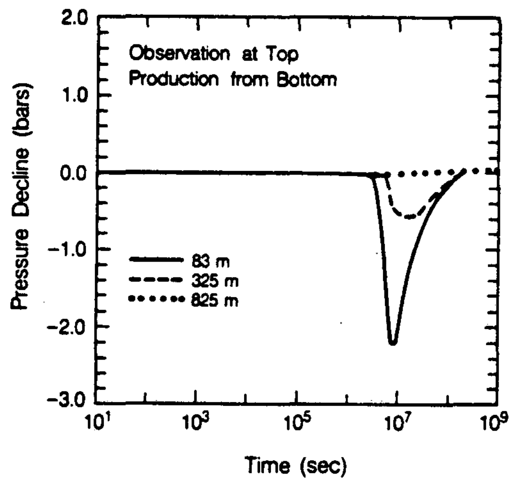

Fig. 5—Pressure transients at shallow observation points located at different radial distances from the well. Fluids are produced from the deep feed zone.

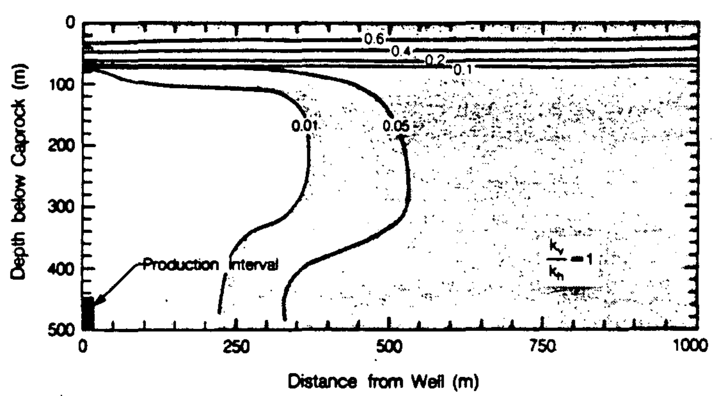

Fig. 6—Vapor saturation contours at the end of the simulation (30 years) for the case of deep production and isotropic permeability.

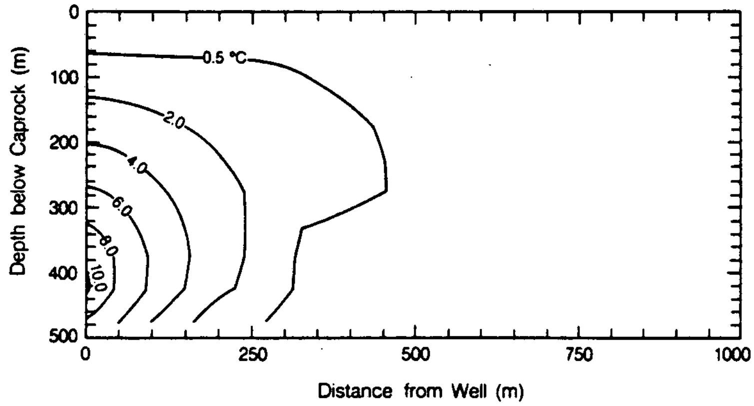

Fig. 7—Total temperature changes in the system at the end of the simulation for the case of deep production and isotropic permeability.

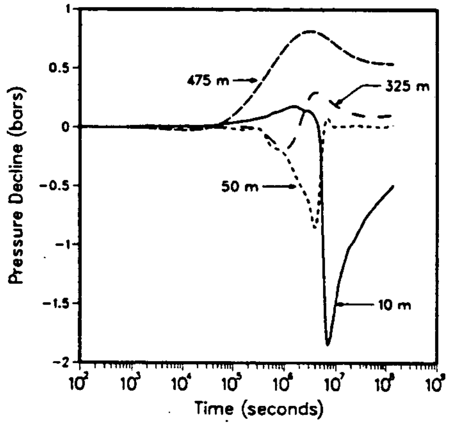

Fig. 8—Pressure declines at four observation depths located a radial distance of 80 m from a deep production zone.

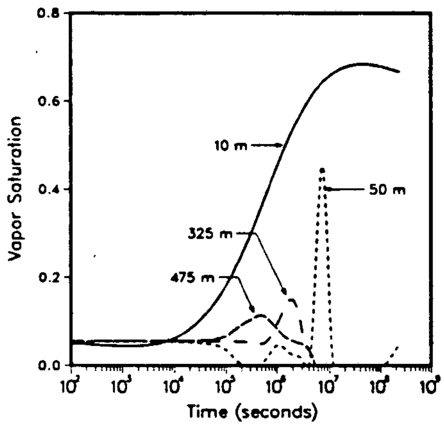

Fig. 9—Vapor saturation vs. time at four observation depths located a radial distance of 80 m from a deep production zone.

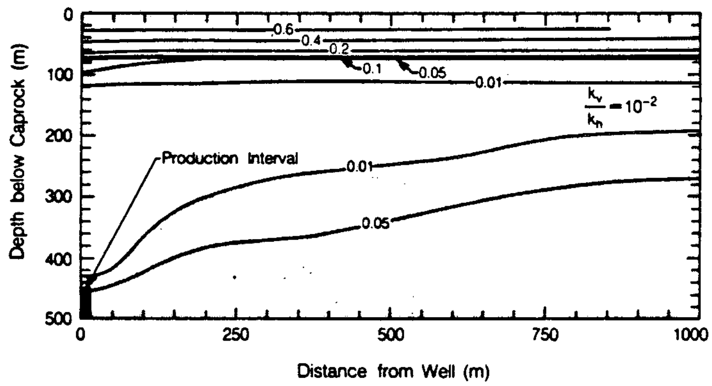

Fig. 10—Vapor saturation contours at the end of the simulation for the case of deep production and permeability anisotropy of 10.

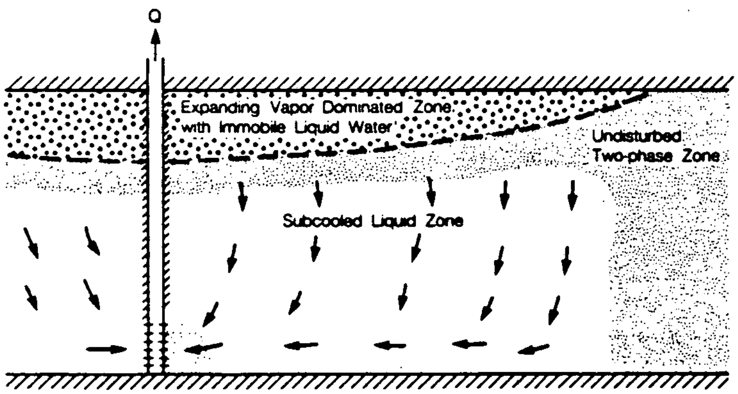

Fig. 11—Schematic model of flow patterns and depletion mechanisms for a well with a deep feed zone.

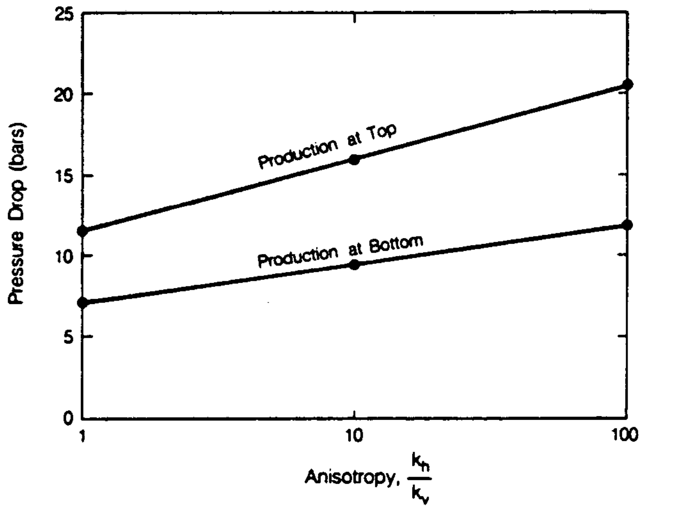

Fig. 12—Relationship between the stabilized pressure decline and permeability anisotropy for cases with deep or shallow feed zones.

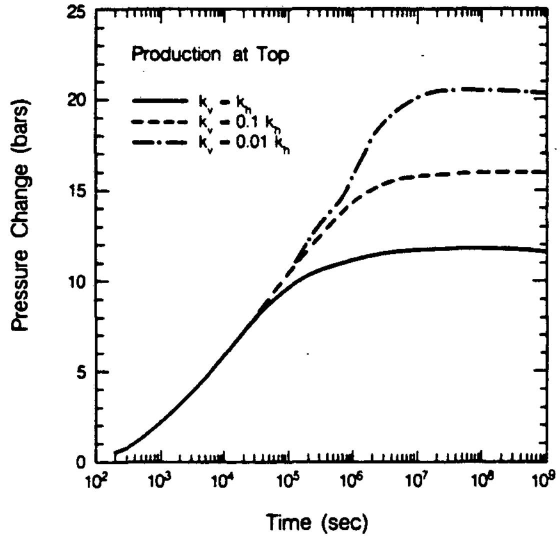

Fig. 13—Pressure decline at the well, when fluids are produced from a shallow feed zone. Different vertical permeabilities are used.

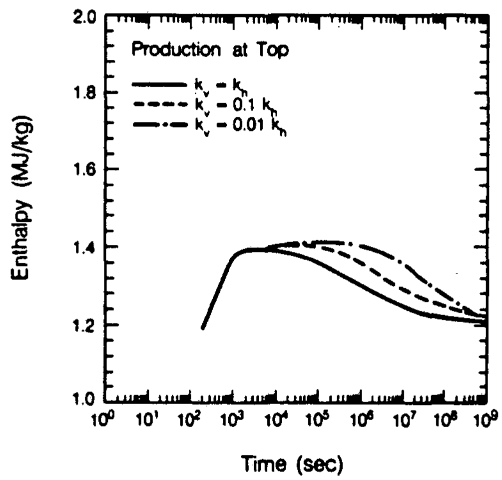

Fig. 14—Flowing enthalpy of the produced fluids for shallow production and various values of the vertical permeability.

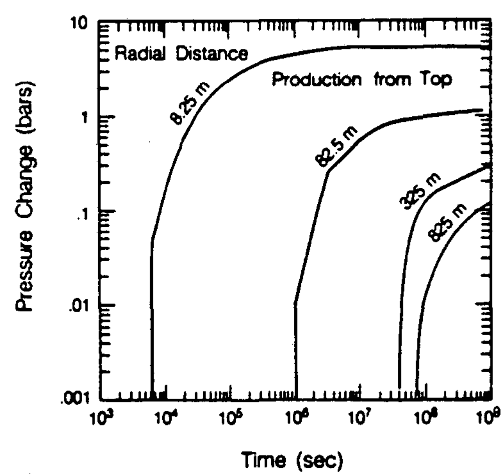

Fig. 15—Pressure transients for shallow observation points located at different radial distances from the well. Fluids are produced from a shallow feed zone.

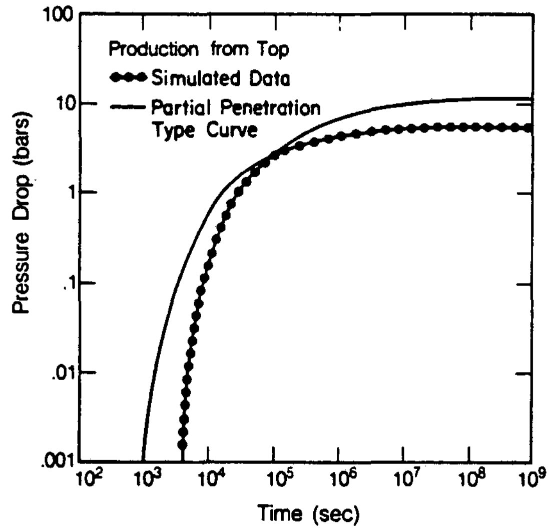

Fig. 16—Partial penetration type curves compared to simulated pressure transients at a radial distance of 83 m from the well. Fluids are produced from a shallow feed zone.

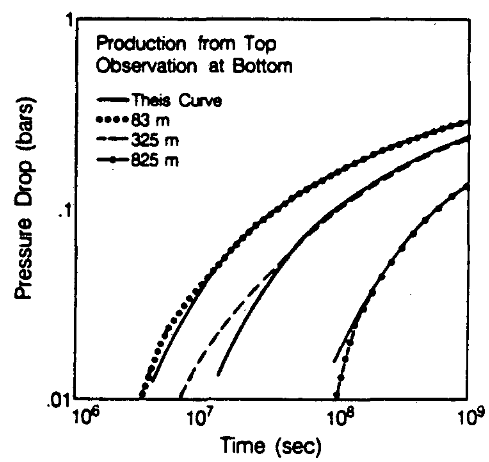

Fig. 17—Simulated pressure transients at deep observation points located at different radial distances from the well. The simulated pressure transients are matched by the Theis curve.